Heinrich events simulated across the glacial

Florian Ziemen, Marie Kapsch, Uwe Mikolajewicz

Max Planck Institute for Meteorology, Hamburg, Germany — florian.ziemen@mpimet.mpg.de

Introduction

Heinrich events are among the most prominent events of climate variability recorded in proxies across the northern hemisphere. They are the archetype of ice sheet – climate interactions on millennial time scales. Nevertheless, the exact mechanisms that cause Heinrich events are still under debate, and their climatic consequences are far from being fully understood. We study the ocean response to Heinrich event ice discharges in a coupled ice sheet model (ISM) atmosphere-ocean-vegetation general circulation model (AOVGCM) framework, where Heinrich events occur as part of the model generated internal variability, and no explicit hosing is necessary. We analyze results from three multi-millenial experiments.

The setup

We use a northern-hemisphere setup of the modified Parallel Ice Sheet Model (mPISM) coupled to the global AOVGCM ECHAM5/MPIOM/LPJ (Ziemen et. al, 2014, **Fig. 1**). The three simulations (**Fig. 4**) were performed fully coupled and with transient orbital and greenhouse gas forcing. To make these multi-millennial simulations feasible, the atmosphere is accelerated by a factor of 10 relative to the other model components using a periodical-synchronous coupling technique.

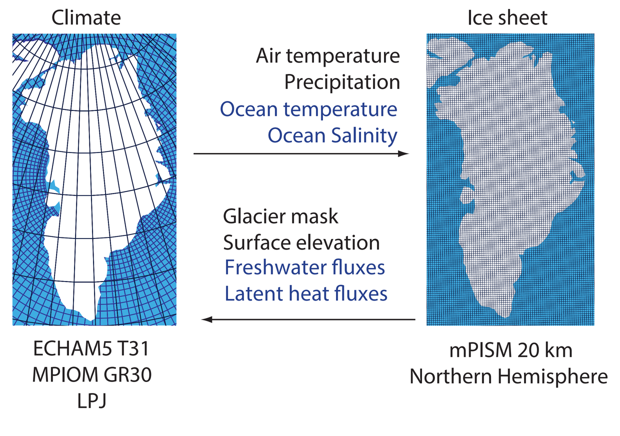

Fig. 1: The coupling scheme.
The model grids are shown for the Greenland area, but cover a larger zone.

Results

The model shows recurring Heinrich events as internal oscillation of the ice sheet (**Fig. 2–4**, for the underlying mechanism see MacAyeal, 1993 and Calov et. al, 2002). They initiate at the separation point of Hudson Strait Ice Stream and its southern tributary, the Ungava Bay Ice Stream, and propagate upstream into the Hudson Bay. The average duration of the events is about 1200 years, and they recur at intervals of about 5000 years, matching basic expectations from reconstructions. To avoid effects of the deglaciation, we focus on the events occurring before 22 kyrs BP (**Fig. 4**). These events show a peak ice discharge of about 0.05 Sv.

The ocean response to the freshwater input shows a substantial variability on centennial time scale. To reduce this short-term variability and obtain more robust results, we average over four events aligned to have the same time of discharge increase (**Figs. 4, 5**). Two of these events are taken from the same long transient experiment. The other two are taken from experiments started from a common ancestor just before a Heinrich event. As the initial ice sheet state of the latter two events is quasi-identical, they show a very similar ice discharge, and – for the ice sheet – cannot be regarded as fully independent ensemble members. Still, the ocean responses differ substantially, allowing to treat them as independent in the ocean analysis.

When the ice enters the ocean, it is modeled as sea ice. The freshly formed sea ice follows the Labrador current (sea ice concentration increase in **Fig. 2**) and melts when it reaches the warm waters of the North Atlantic. Here it releases its freshwater content that then follows the eastward route of the North Atlantic Current (**Figs. 6, 8**). The freshwater reduces the mixed layer depth, and the North Atlantic Deep Water cell strength (**Figs. 6–9**). With less heat supply from below, the sea surface temperature drops (**Fig. 9**). Despite a reduction in wind driven transport, the Subpolar Gyre strengthens (**Figs. 10, 11**). The surface air temperature decrease is strongest in the area with increased sea ice cover (**Figs. 2, 12**). From there it spreads eastward across Eurasia and large parts of the Arctic. The ITCZ over the Atlantic and Africa shifts southward (**Fig. 13**).

After the surge, sea surface salinity and NADW cell strength quickly recover (**Figs. 6–8**). The lower ice sheet (**Fig. 3**) causes a more zonal jet stream (not shown) and a stronger reduction in wind driven transport (**Fig. 11**). The subpolar Gyre weakens (**Fig. 10**), and the sea ice margin in the Irminger Basin and the Nordic Seas advances (**Fig. 3**). The mixed layer depth remains reduced (compare **Figs. 8, 9**). The sea surface temperature and the surface air temperature partly recover (**Figs. 9, 12**). The dipole pattern in the tropical Atlantic precipitation reduces to a precipitation increase in the south, while over Africa and the Indian ocean, the dipole structure remains intact (**Fig. 13**).

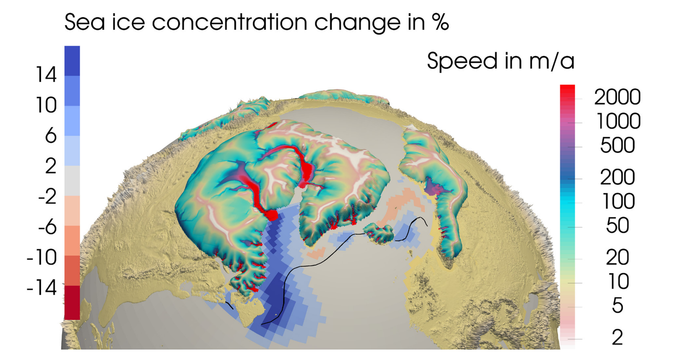

Fig. 2: Ice velocities at year 450 of the surge.
Over the ocean, colors mark the sea ice concentration change compared to the reference period. The black isoline marks 15% sea ice concentration before the surge. Vertical exaggeration: 100. Present-day topography is displayed around the ice sheets for orientation. Average of all four events.

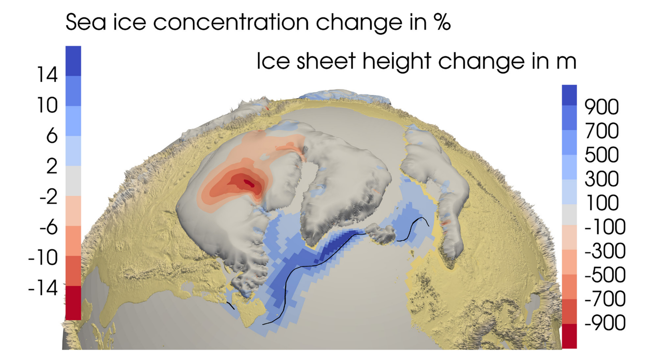

Fig. 3: Ice surface elevation change at year 1250.
Over the ocean, colors mark the sea ice concentration change compared to the reference period. The black isoline marks 15% sea ice concentration before the surge. Average of all four events.

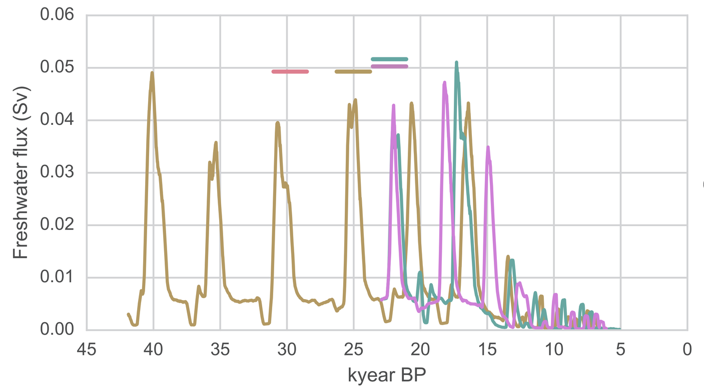

Fig. 4 Hudson Strait ice discharge
300 year running mean of the Hudson Strait ice discharge in all simulations. The events used in the analysis are marked.

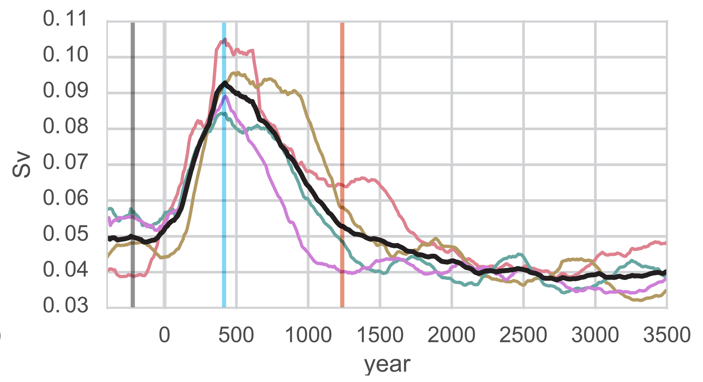

Fig. 5: Net Labrador Sea Freshwater flux
300 year running mean of the net surface freshwater flux into the Labrador Sea. Individual events are aligned to identical ice discharge increase (not shown) and are shown in colors. The ensemble mean is shown in black.

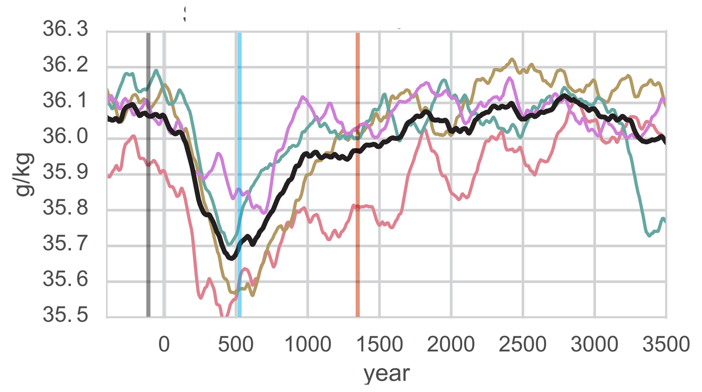

Fig. 6: North Atlantic sea surface salinity
300 year running mean over the open North Atlantic north of about 30°N.

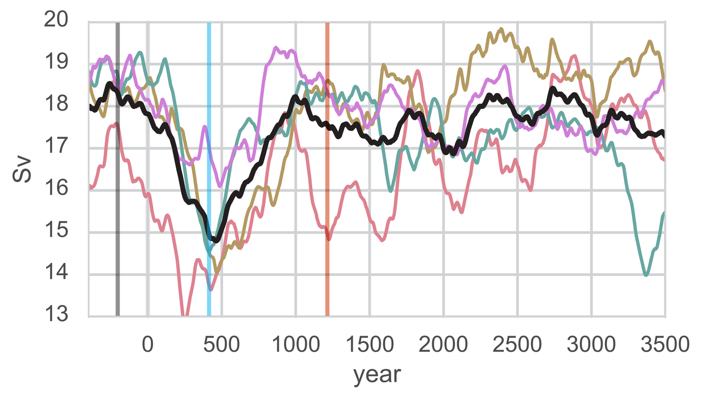

Fig. 7: North Atlantic Deep Water cell strength
300 year running mean of the maximum cell strength at 30°N.

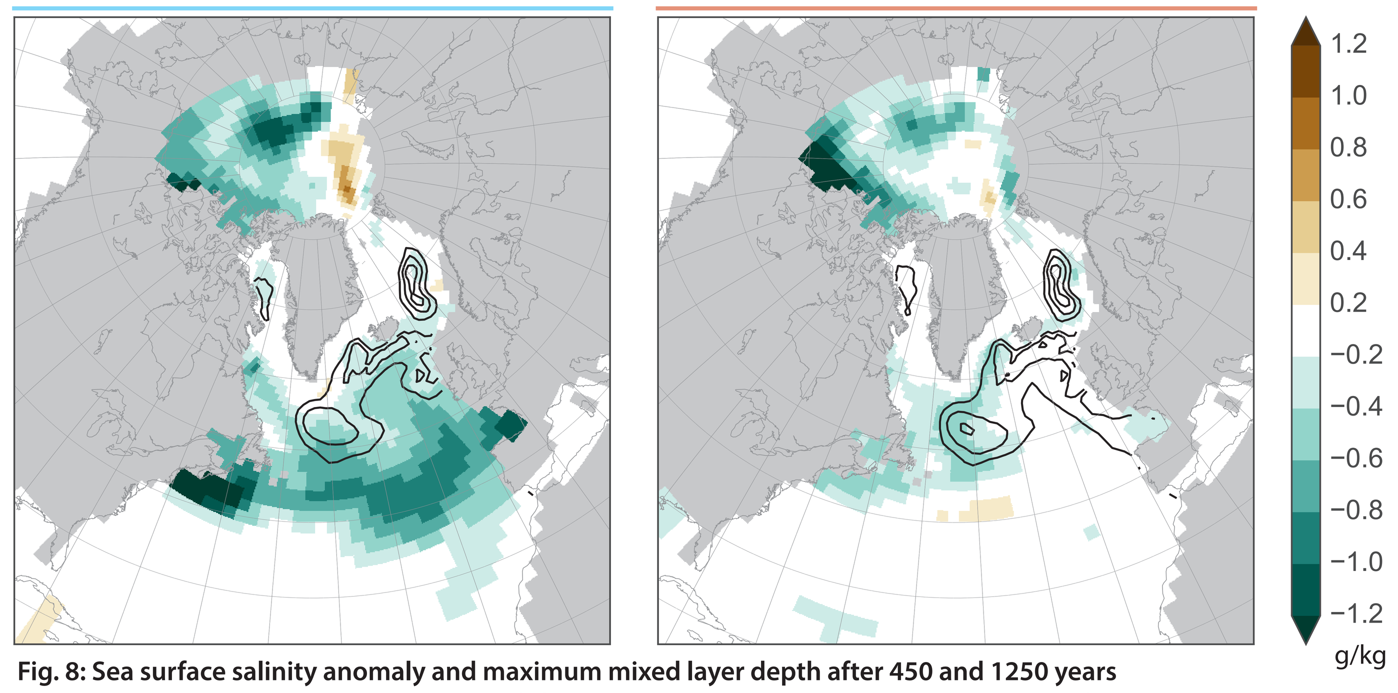

Fig. 8: Sea surface salinity anomaly and maximum mixed layer depth after 450 and 1250 years
300 year means centered around years 450 (left) and 1250 (right). Around year 450, the anomaly spreads out across the whole North Atlantic. There is little effect in the East Greenland current and the Labrador Sea. Around year 1250, the anomaly is focused on the Newfoundland Basin. The effect in the Eastern North Atlantic is reduced. However, the mixed layer remains shallow. For the mixed layer depth before the event, see **Fig. 9**.

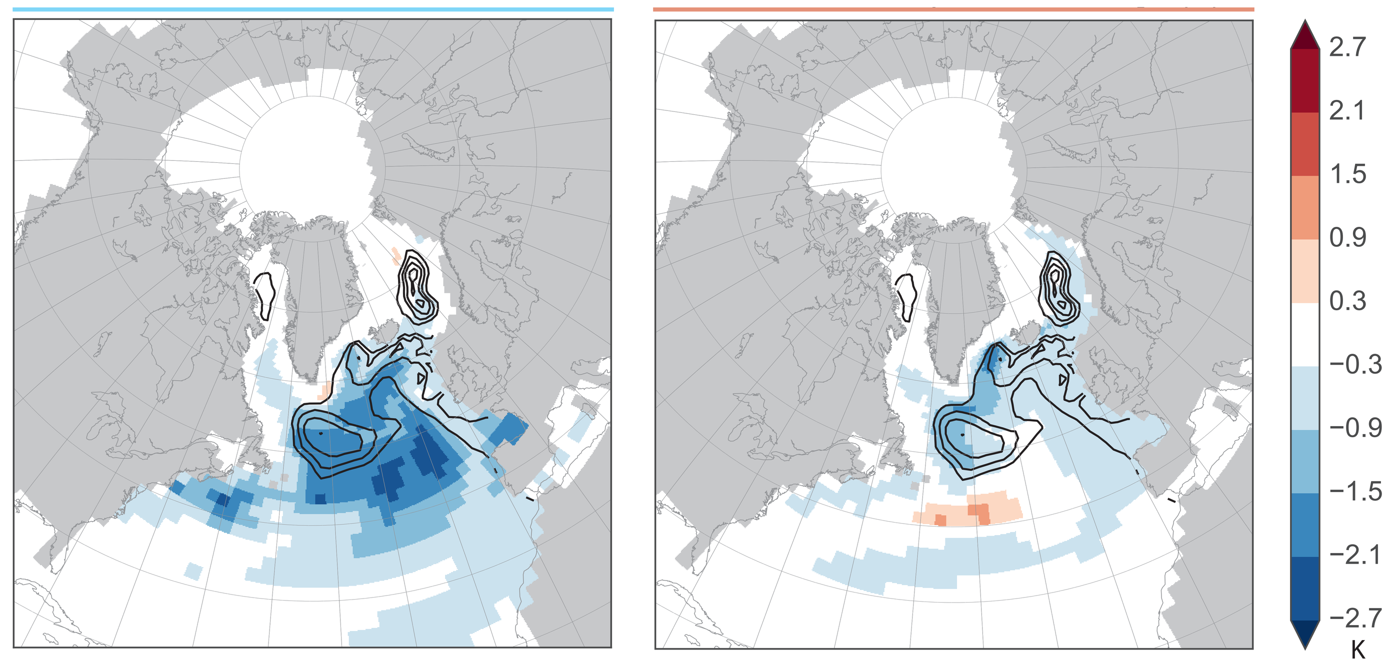

Fig. 9: Sea surface temperature anomaly after 450 and 1250 years.
300 year means centered around years 450 (left) and 1250 (right). The overlay shows the mixed layer depth before the event on 500 m levels. Around year 450, the cooling spreads wide into the east, while around year 1250 it is weaker and shifted to the north. The weakening matches with the pattern in the SSS (**Fig. 8**). The northward shift matches with increased sea ice cover in the Nordic Seas (**Fig. 3**). The warming at 40°N, 40°W is a result of a more northerly route of the North Atlantic Current (**Fig. 10**).

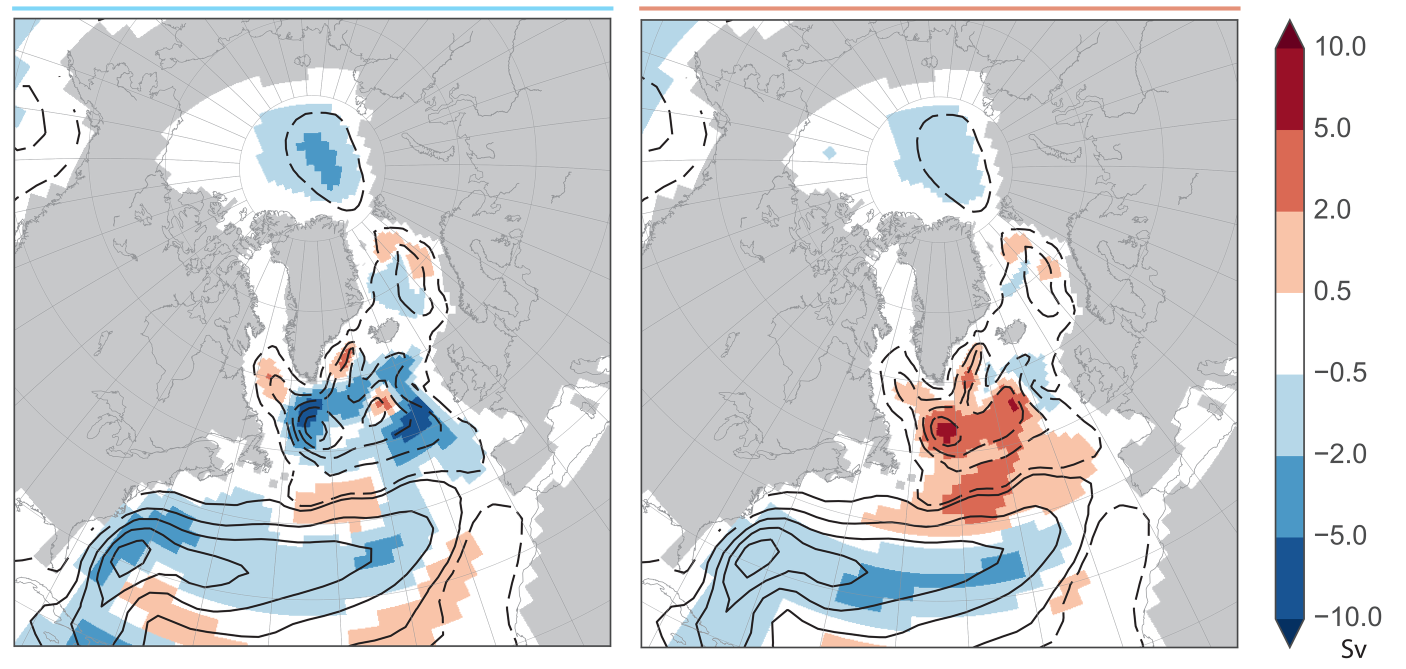

Fig. 10: Barotropic stream function anomaly after 450 and 1250 years
300 year means centered around years 450 (left) and 1250 (right). Overlays show the barotropic stream function at contour levels of ±1 Sv and multiples of 10 Sv. Around year 450, the Subpolar Gyre is strengthened while the North Atlantic Current is slightly weakened. Around year 1250, both gyres are weakened and the North Atlantic Current takes a slightly more northerly path. The weakening of the Subpolar Gyre is partly caused by a reduced Sverdrup transport (**Fig. 11**, different colorscale!).

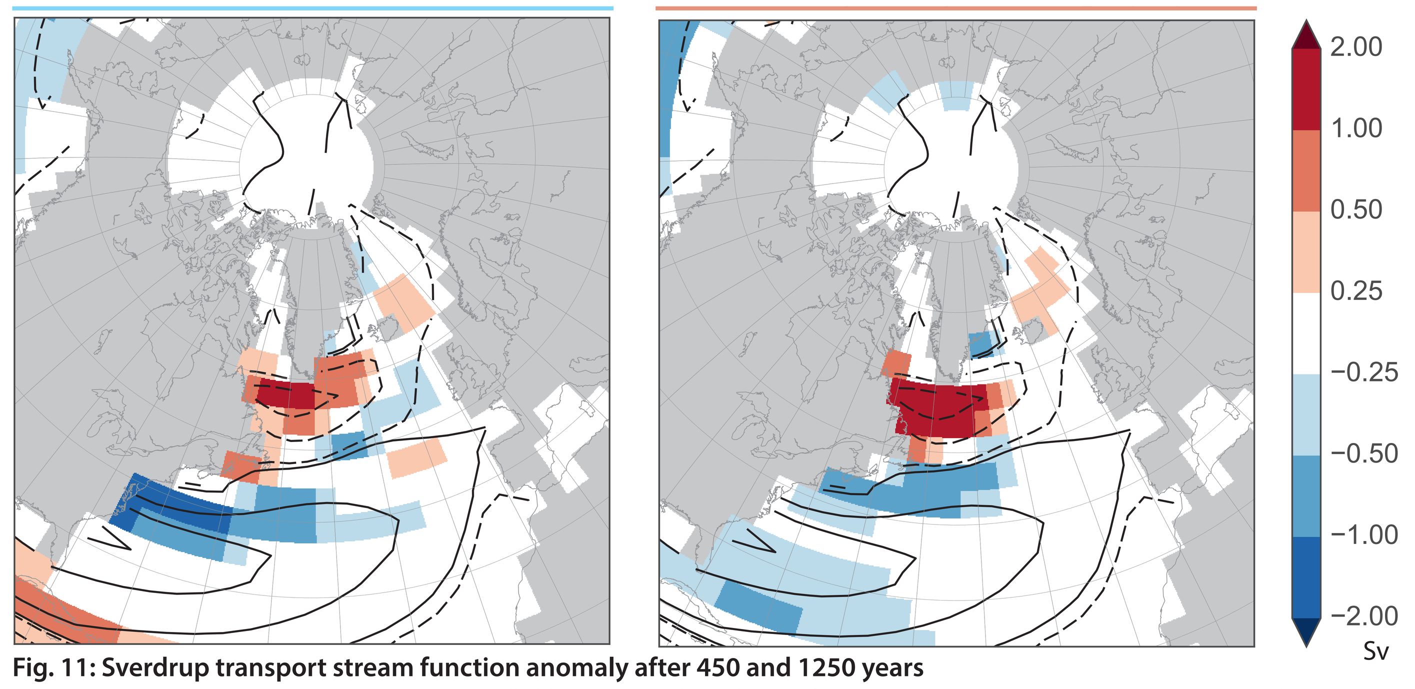

Fig. 11: Sverdrup transport stream function anomaly after 450 and 1250 years
300 year means centered around years 450 (left) and 1250 (right). Overlays show the Sverdrup transport stream function averaged over the 400 years before the event at contour levels of ±1 Sv and multiples of 10 Sv. Around year 450, the Sverdrup transport in the Subpolar Gyre is already reduced, while the gyre strength increases (**Fig. 10**, different color scale!). Around year 1250, the Sverdrup contribution to the Subpolar Gyre is weakened further and so is the gyre.

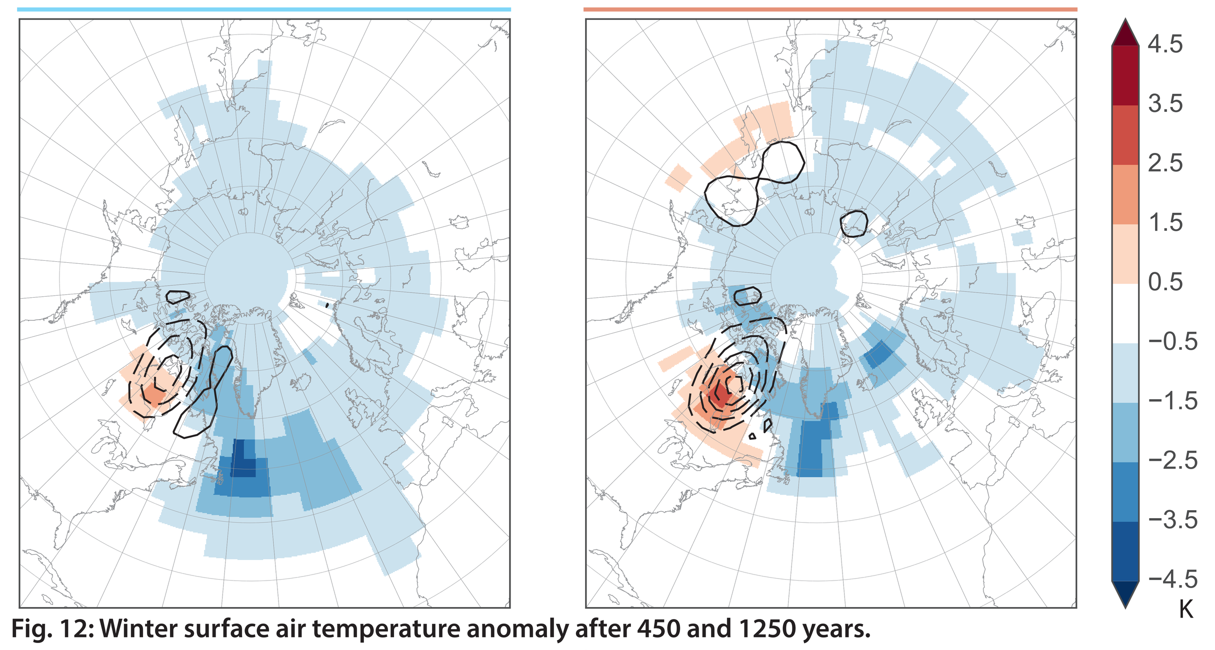

Fig. 12: Winter surface air temperature anomaly after 450 and 1250 years.
300 year DJF means centered around years 450 (left) and 1250 (right). The overlays show the ice sheet surface elevation change as seen by ECHAM5 on levels of ±50, 150, 250, … m. Dashed lines mark elevation decrease. The cooling over the North Atlantic and the Nordic Seas is strongly related to the sea ice changes (**Figs. 2, 3**). The warming over the Laurentide Ice Sheet is a consequence of the surface elevation decrease, but only partially can be explained by the atmospheric lapse rate. This is shown by the mismatch between the patterns of temperature and elevation changes.

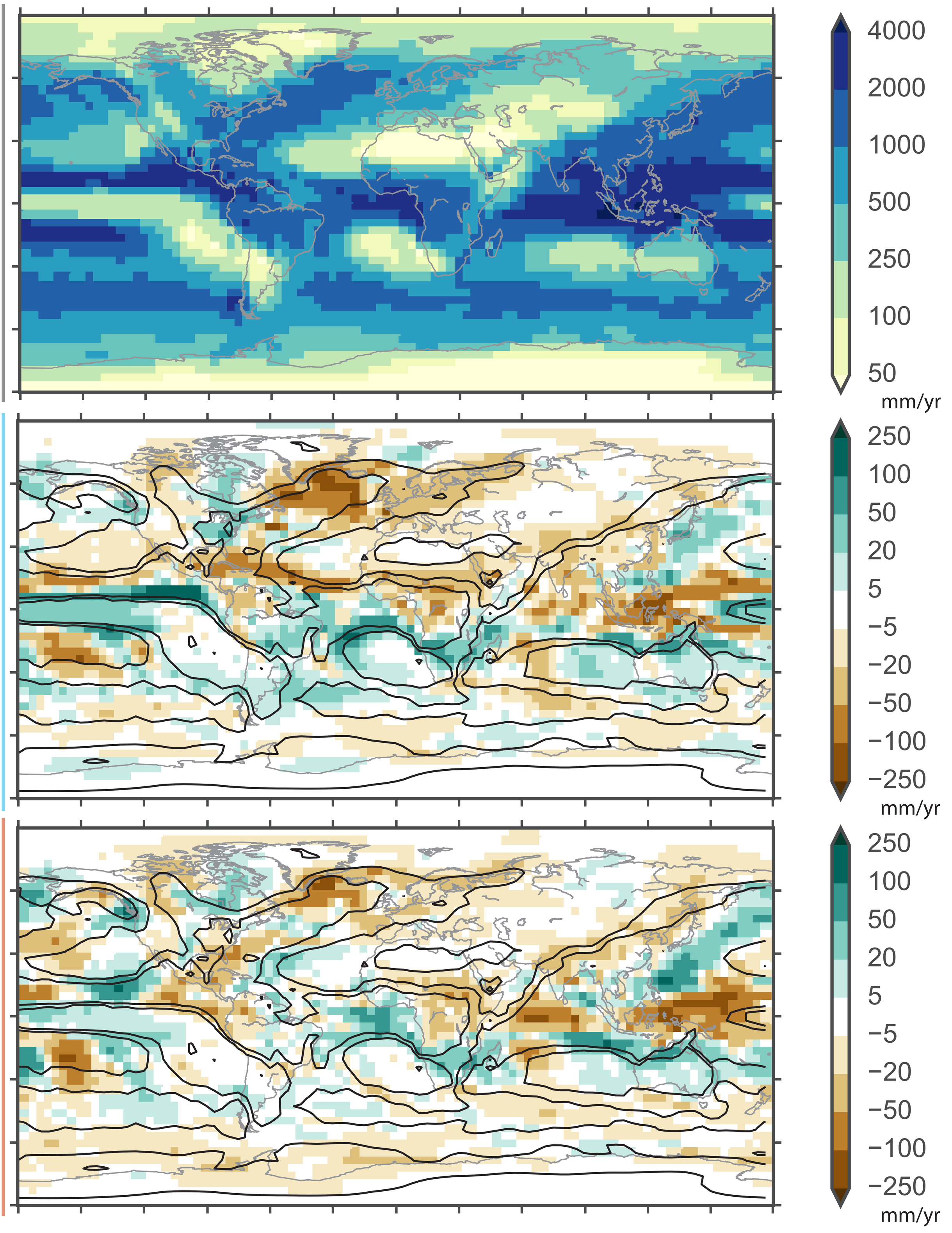

Fig. 13: Precipitation before the event, and anomalies after 450 and 1250 years.
Precipitation before the event averaged over 400 years (top). 300 year mean anomalies centered around years 450 (middle) and 1250 (bottom). The overlays show the precipitation before the event on levels of 50, 500, and 1000 mm/yr.

Calov, R., Ganopolski, A., Petoukhov, V., Claussen, M., & Greve, R. (2002). Large-scale instabilities of the Laurentide ice sheet simulated in a fully coupled climate-system model. GRL.
MacAyeal, D. R. (1993). Binge/Purge Oscillations of the Laurentide Ice Sheet as a Cause of the North Atlantic's Heinrich Events. Paleoceanography.
Ziemen, F. A., Rodehacke, C. B., & Mikolajewicz, U. (2014). Coupled ice sheet–climate modeling under glacial and pre-industrial boundary conditions. Climate of the Past.

Max-Planck-Institut für Meteorologie
SPONSORED BY THE Federal Ministry of Education and Research
PALMOD GERMAN CLIMATE MODELING INITIATIVE